LBL-18535
c.2

Lawrence Berkeley Laboratory
UNIVERSITY OF CALIFORNIA

RECEIVED
LAWRENCE
BERKELEY LABORATORY
NOV 1 1984
LIBRARY AND
DOCUMENTS SECTION

APPLIED SCIENCE DIVISION

Presented at the Western States Section/The
Combustion Institute 1984 Fall Meeting,
Stanford University, Stanford, CA,
October 22-23, 1984

A COMPARATIVE STUDY OF COMBUSTION IN UNVENTED SPACE HEATING DEVICES

T. Lionel, R.J. Martin, and N.J. Brown

October 1984

TWO-WEEK LOAN COPY
This is a Library Circulating Copy
which may be borrowed for two weeks.

APPLIED SCIENCE
DIVISION

LBL-18535
c.2

Prepared for the U.S. Department of Energy under Contract DE-AC03-76SF00098

DISCLAIMER

This document was prepared as an account of work sponsored by the United States Government. While this document is believed to contain correct information, neither the United States Government nor any agency thereof, nor the Regents of the University of California, nor any of their employees, makes any warranty, express or implied, or assumes any legal responsibility for the accuracy, completeness, or usefulness of any information, apparatus, product, or process disclosed, or represents that its use would not infringe privately owned rights. Reference herein to any specific commercial product, process, or service by its trade name, trademark, manufacturer, or otherwise, does not necessarily constitute or imply its endorsement, recommendation, or favoring by the United States Government or any agency thereof, or the Regents of the University of California. The views and opinions of authors expressed herein do not necessarily state or reflect those of the United States Government or any agency thereof or the Regents of the University of California.

To be presented at the Western States Section/
The Combustion Institute 1984 Fall Meeting, at
Stanford University, Stanford, CA, October 22-23, 1984.
Paper No. 84-57.

A COMPARATIVE STUDY OF COMBUSTION IN UNVENTED SPACE HEATING DEVICES

T. Lionel, R.J. Martin, and N.J. Brown

Applied Science Division
Lawrence Berkeley Laboratory
University of California
Berkeley, CA 94720

This research was supported by the Assistant Secretary of Conservation and Renewable Energy, Office of Energy Systems Research, Energy Conservation and Utilization Technology Division of the U.S. Department of Energy, under Contract No. DE-AC03-76SF00098.

ABSTRACT

The combustion characteristics of radiant, convective, and multi-stage kerosene heaters have been determined and compared. Two types of experiments were conducted. In the first of these, composition and temperature were measured as a function of axial position in the heater to determine the progress of combustion. In the second type, composition, fuel consumption rate, temperature, pressure, and exhaust stream mass flow rate were measured in an exhaust manifold to ascertain the effect of heater type and heater operating conditions on exhaust gas composition. Fuel consumption was sensitive to wick height, wick age, and volume of fuel in the tank. Heater design strongly influenced emission concentrations. The multi-stage heater had the smallest concentration of CO and intermediate concentrations of NO_x. The radiant heater had the largest concentrations of CO and smallest NO_x concentrations. The convective heater had the greatest NO_x concentrations. Results were compared with chamber and other laboratory studies, and agreement among the various studies was found to be quite satisfactory.

I. INTRODUCTION

Energy conservation can be achieved in the home environment by modifications of ventilation, insulation and heating. The use of space heaters in residences has become more popular as the cost of central heating systems has increased. Kerosene heaters offer a truly portable alternative to electric, natural gas or oil-fired heaters, however their unvented design necessitates consideration of the effects of combustion emissions in the indoor environment. The rate of air infiltration is closely coupled to emission levels in affecting the indoor air quality.

Descriptions of the emissions produced by kerosene heaters have involved three types of experiments: laboratory studies characterizing exhaust concentrations (Yamanaka, 1979), environmental chamber studies (Kweller, 1980; Leaderer, 1982; Traynor, 1983), and field studies in houses (Clarkson, 1984; Leaderer, 1984; Yamanaka, 1984). The indoor air pollutants carbon monoxide (CO), sulfur dioxide (SO_2), oxides of nitrogen ($NO_x = NO_2 + NO$), carbon dioxide (CO_2), unburned hydrocarbons and particulates have been detected.

Emissions of NO_x were first detected in laboratory studies (Yamanaka, 1979) in the exhaust of radiant and convective types of kerosene heaters. In order to simulate the operation of kerosene heaters, environmental chamber "test rooms" were constructed to control ventilation rates to values expected in residences. In two separate chamber studies (Leaderer, 1982; Traynor, 1983), occupational health standards for CO_2 and ambient air quality standards for NO_2 were exceeded for both radiant and convective types of kerosene heaters. Radiant heaters also produced cautionary levels of CO in small rooms. Leaderer measured levels of SO_2 in excess of ambient air quality standards. Traynor et al. observed that reducing wick heights led to reduced rates of combustion but increased CO and formaldehyde emissions rates.

The next step in characterization of kerosene heater pollutant emissions

was to examine their concentrations in actual residences. In a typical Japanese living room, the decay process of NO_2 generated from a convective heater was found to follow first-order kinetics (Yamanaka, 1984). A study in a Canadian test house (Clarkson, 1984) indicated that operation in large ventilated rooms produced more acceptable, lower concentrations of CO and NO_x than in small rooms. An extensive study (Leaderer, 1984) of over 300 residences in Connecticut indicated that concentrations of CO_2, NO_2 and SO_2 exceeded ambient standards during peak exposures. In homes with an additional combustion source such as a gas stove or a second kerosene heater, higher NO_2 concentrations were detected.

In this paper we will compare the combustion characteristics of radiant, convective, and multi-stage kerosene heaters. All heaters have a wick (first stage) to introduce kerosene to the primary combustion chamber (second stage) where much of the combustion occurs. Experiments have been performed to ascertain the effects of heater design and heater operating conditions on exhaust gas compostion.

II. Experimental

A. Description of Apparatus

An exhaust and sampling manifold has been designed and is positioned above the kerosene heater which completely mixes the products of combustion while producing no effect upon the burning characteristics. Measurements were carried out with each heater positioned such that the top was even with the bottom of the exhaust manifold. Probe ports are located in the manifold at three different axial positions, five cm apart. Each position has two tapped ports 90° apart to permit probing at different radial positions. In addition, samples can be obtained from inside the heaters by inserting probes through openings in the structure. The multi-stage heater was modified to allow vertical probing through one of three tapped ports located at and near the heater top. Probe repositioning is possible while a heater is operating; however, the error in positioning is approximately 0.2 mm in the sampling manifold and approximately 2.0 mm inside a heater.

Samples are withdrawn through probes constructed from 3.0 mm O.D., 2.0 mm I.D. quartz tubing with tips narrowed to an orifice diameter of 0.3 to 0.5 mm. In general, straight probes were used, with the exception of sampling done at the top of the second stage of the multi-stage heater where it was necessary to bend the quartz tubing to reach the flame zone. The probes are connected by filtered heated teflon lines to either a gas chromatograph, a non-dispersive infra-red analyzer, a chemiluminescence analyzer or a pulsed fluorescence analyzer. Each analyzer is equipped with pumps for sample extraction. Combustion products detected are hydrocarbons, CO_2, NO_2, SO_2, CO, NO, O_2, and N_2. Additional diagnostic information is obtained from a series of measurements characterizing physical parameters, e.g., temperature, pressure, fuel consumption, and flow velocity.

Fuel uniformity was assured by the purchase of a large quantity of kerosene (Union Oil K-1). The fuel was analyzed at the University of California microchemical analysis and mass spectrometer laboratories. The elemental composition was determined yielding a kerosene carbon-hydrogen mass ratio of 6.38, and a sulfur content of 0.04% by weight. The limit of detectability for nitrogen was 0.01 mass percent, nitrogen in excess of this amount was not reported.

B. **Chemical Analysis**

Oxides of nitrogen are measured with a chemiluminescence analyzer (CLA), Thermo-Electron Model 14A, modified with heated sample capillaries to minimize H_2O condensation. Calibration was carried out with standards of NO_2 in N_2, NO in N_2, and a very dilute mixture of the two oxides in N_2. These standards were independently verified by the Industrial Hygiene Laboratory of the California State Department of Health . Analyzer linearity was checked by dilution of standard mixtures with N_2 to prepare concentrations down to the very low ppm range. The measurements of NO_x and NO made on the kerosene heater are sensitive to within 0.1 ppm.

Total hydrocarbons, CO_2, CO, O_2, and N_2 are measured with a gas chromatograph (GC), Hewlett-Packard Model 5880A. In order to measure CO_2, CO, O_2, and N_2, a temperature programmed series/bypass configuration was prepared with Porapak Q and Molecular Sieve 5A columns attached to a thermal conductivity detector. At the same time, samples were analyzed for total hydrocarbon content with a flame ionization detector. Carbon monoxide was only detectable to approximately 100 ppm by this method. Water was estimated from the stoichiometry of kerosene combustion. Both pure gases and prepared mixtures simulating combustion exhaust concentrations were used to calibrate for atmospheric pressure sampling. Chromatograms of gas samples were

integrated and compared with the calibrations automatically; sequential injection, elution, and storage of data was also controlled by programming the G.C. The precision of the gas chromatograph measurements was better than 2% for oxygen and nitrogen at their atmospheric concentration levels. At levels found in the emissions, CO_2 and CO can be detected to better than 2% precision. Hydrocarbons can be detected at better than 3% precision.

Carbon monoxide is detected in the very low ppm range with a non-dispersive infra-red analyzer (NDIR), Bendix Model 8501-5CA. Calibration was achieved by comparison with a standard of CO in N_2. The concentration of the calibration gas was also verified at the Industrial Hygiene Laboratory of the Department of Health. Analyzer linearity was again confirmed by dilution with N_2 and the sensitivity of measurements of CO was within 0.1 ppm.

Sulfur dioxide is measured with a pulsed fluorescence analyzer, Thermo-Electron Series 40, calibrating with standards of SO_2 in N_2. It was necessary to ensure that H_2O present in the combustion emissions did not interfere with detection by solution of SO_2 or by quenching of fluorescence (Lucas, 1984).

C. Physical Measurements

Fuel consumption rate was measured gravimetrically by a triple-beam balance, with precision to one gram in 20 kilograms. Temperatures were measured in both the exhaust manifold and in the heater interiors. Chromel-Alumel thermocouples, with exposed junctions and 1.0 mm bead diameters were used for all temperature measurements. Reported data are not corrected for radiation or conduction losses. Radiation error will be completely negligible in the exhaust manifold where temperatures are below 520 K. In the heater combustion chambers, where peak temperatures do not exceed 1120 K, radiation error is likely to be less than 10 degrees. In the third stage of the multi-stage heater, temperatures are expected to reach 1470 K at the flame front.

Here the radiation loss from the thermocouple junction and particulate adhesion to the thermocouples could induce much larger measurement errors. Static pressures in the naturally-aspirated heater and in the exhaust stack varied less than 0.02 mm Hg from the local barometric pressure of approximately 740 mm Hg. Air flow rates were not monitored since air is entrained into all three kerosene heaters at the base, and above the wick in the convective and multi-stage designs. The heater would have had to be placed in a fairly large chamber to monitor air in-flow and not alter the combustion characteristics. Exhaust gas mass flow rate in the exhaust manifold was determined from measured velocities, temperatures, and pressures. Velocity was measured by a 3.17 mm O.D. Pitot probe aligned with the flow at various locations in the exit plane of the manifold. Differential pressures were measured with a Dwyer-Microtector manometer. Precision of the manometer is 0.01 mm of the water column height, resulting in better than 10% precision for the calculated velocity.

III. RESULTS AND DISCUSSION

Experiments were performed on radiant, convective and multi-stage heaters (see Figure 1) to acquire an understanding of the combustion occuring. The experiments were of two types. In the first type composition and temperature were measured at different spatial locations in the heater to determine the progress of combustion as a function of axial position. In the second type, composition, temperature, pressure, and exhaust gas mass flow rate were measured in an exhaust manifold to ascertain the effect of heater type and heater operating conditions on exhaust gas compostion.

It is useful to indicate the overall stoichiometry of kerosene burning. The balanced chemical equation for complete combustion is:

$$C_{13}H_{24.4} + (19.1+x)(O_2+3.76N_2) \longrightarrow 13CO_2 + 12.2H_2O + xO_2 + (71.8+3.76x)N_2 \qquad (1)$$

The chemical formula for kerosene is determined from the elemental analysis and the fact that the average number of carbon atoms per hydrocarbon in kerosene is 13. The symbol x in the above balanced reaction is the number of moles of excess oxygen present, which can be determined from the measured concentrations of N_2, O_2, and CO_2 after assuming complete combustion.

A. Combustion Characteristics

The kerosene heaters selected for study consist of three major parts. The first of these is the wick, which is a circular ring of woven fiberglass, where fuel evaporation occurs. Temperatures immediately above the wick area are on the order of 470 K. The wick is enclosed by two concentric perforated metal cylinders, which are in turn enclosed by a pyrex cylinder in the radiant and multi-stage heaters. This second stage assembly is called a combustion chamber and is illustrated schematically for the multi-stage heater in Figure 2. A significant amount of combustion occurs in the region between the metal

cylinders. Temperatures in the chamber rise quickly from approximately 470 K directly over the wick to 1070 K and remain between 1070 and 1170 K up to the top of the cylinder. The third section of the heater functions to mix the products of combustion and increase the residence time available for combustion. In the radiant design, this section is the space surrounding the combustion chamber and enclosed on all but one side by reflective surfaces to radiate heat outward. In the convective and multi-stage heaters, the third section is a closed cylinder, either constructed of metal and enclosing the combustion chamber (convective), or constructed of glass and placed on top of it (multi-stage). Within the third section, products of incomplete combustion remaining after second stage burning, are converted to CO_2 and H_2O. The peak temperature in the multi-stage heater's third section is higher than the second stage values. Mixing is improved and the opportunity for more complete combustion is enhanced. Temperatures in the third stage are variable and dependent upon the degree of mixing of dilution air. Temperatures as high as 1332 K have been measured near the flame contours. Above the contours, at the top of this section, temperatures are approximately 870 K in both the convective and multi-stage heaters.

Air and fuel mixing in these and other heaters in the U.S. marketplace is accomplished by free convection. Most of the air enters from a series of holes located at the heater base, below the wick. A large column of air enters within the area enclosed by the wick, and a large volume fraction of this is not mixed with fuel or products of combustion until the third section or later. Air is also entrained from the base of the heater around the exterior wall of the outermost metal cylinder and this flows upward and is used for combustion in the second stage combustion chamber and to cool the exterior walls of the heater. In the multi-stage heater, additional air is introduced through holes located near the boundary of the second and third stages. Mixing of fuel and

oxidizer is enhanced by various flow diversion structures at the top of the combustion chamber ranging from a circular coil and umbrella-shape in the radiant heater to a cone and disc in the multi-stage heater. In the convective and multi-stage designs, flaming combustion occurs in the third stage, about the periphery of the flow diversion disc. Mixing times are long and the flow field where combustion occurs is characterized by regions of steep gradients. A series of temperature measurements in the multi-stage heater indicate that the flow field is axially symmetric over the wick, in most of the second stage, and at the end of the third stage, but not at the interface between the second and third stages.

An understanding of the combustion characteristics of the newer design multi-stage heater can be obtained by reviewing the results of experiments of the first type which are summarized in Table I. In these experiments, hydrocarbons, CO_2, NO_2, NO, CO, N_2, and O_2 were measured. The quantity ϕ, the equivalence ratio, is determined from measured CO_2, O_2 and N_2 and is defined in the usual way, $(\text{fuel/air})/(\text{fuel/air})_{\text{stoichiometric}}$. The ratio is somewhat in error when CO concentrations are appreciable. The tabulated value is computed after assuming complete combustion, and it is useful for quantifying the large amount of dilution air present. The data in Table I were taken at a fixed radial position from variable axial positions in the heater, as shown in Figure 3. The axial profile, which will be described, is in a region of strong gradients where the composition and temperature probes are likely to sample a composition which is an average over more than one probe diameter.

The first entry in Table I is representative of the area between, and near the top of, the concentric cylinders where the temperature is approximately 1070 K. It was not possible to measure composition at lower axial positions than this because of hydrocarbon interference. The hydrocarbons, present at

the lower axial positions, consist of a wide range of products of incompletely combusted kerosene which condense in probes and make quantitative analysis of the gaseous products of combustion very difficult. Relatively large CO and hydrocarbon concentrations are found, indicating incomplete combustion at this location (position 1 in Figure 3). A large NO_x concentration results from the formation of most of the NO_x before the third stage, and the contributing NO_2 and NO concentrations are nearly equal. The second entry in the table indicates the conditions toward the center of the heater out of the flaming zone and influenced by the central air column dilution. The third entry is representative of composition at the beginning of the convection section just below and outside the flame. Here products of combustion have been mixed with a relatively large amount of dilution air as reflected in the large value for the equivalence ratio. Note that the CO concentration is still appreciable. The entry designated 4 is for a sample taken from the convective section inside the flame contour, where hydrocarbons and CO are relatively abundant and the NO_x is present mainly as NO. Compositions are next indicated at position 5, above the flame contour in a region of more dilution than the previous entry. Within experimental error, the data reveal that the $CO \rightarrow CO_2$ burnout occurs between positions 4 and 6. The next four entries in the table are to within experimental error nearly equivalent. They indicate that 1) combustion is complete, with no measureable CO and hydrocarbons present (detected with the GC), and 2) after passing through the flame zone, the NO_x along this axis is mostly present as NO.

To investigate symmetry inside the third stage of the multi-stage heater, measurements were made at various points around an axis, at fixed radial positions above the flame zone. Figure 3 indicates the positioning of the probe for these experiments, corresponding to the axial locations designated by positions 7 and 9. Compositions were the same as positions 7 and 9 in Table I

and axial symmetry was found. Examination of Table II, where these data are summarized, reveals that the products of combustion are quite well mixed before reaching the top of the third stage. Combustion is also nearly complete since hydrocarbon and CO concentrations were below the limit of detectability with the GC.

B. Measurements in the Exhaust Manifold

Prior to conducting experiments to determine the effect of operating parameters on final gas composition, measurements were performed to verify reproducibility of the heater combustion and to determine the uniformity of conditions in the sampling manifold. Early measurements were performed with the exhaust manifold open to the laboratory above the level of the sample ports; in later measurements, the manifold was connected to an externally directed vent. Radial temperature and velocity profiles were measured in the exhaust duct, to provide an indication that conditions were uniform. The temperature profile, shown in Figure 4, was measured 15.2 cm downstream of the manifold inlet. The profile was nearly uniform across much of the central region, and exhibited steeper gradients near the wall. The shape of the profile is typical of turbulent flow in circular ducts. When the exhaust manifold was open, flow rates measured with a Pitot tube were at the lower limit, and these had an uncertainty of $\pm 10\%$. However when the exhaust was directed externally and a new Pitot tube and static pressure probe were used, the measured values were very close to flow rates computed from fuel consumption and measured CO_2 concentrations.

All three heaters are designed to allow the wick position to be altered to adjust the heat output. Adjustment is over a much greater range in the multi-stage heater than with the radiant and convective heaters and is designed to be reproducible by the use of a graduated scale next to the wick height adjustment.

A good indication that the heater operates reproducibly is the consistency of fuel consumption rate measurements. Table III summarizes fuel consumption rates for three different heaters, and shows the effect of different wick heights on the fuel consumption data. The largest measured deviation from the mean fuel consumption rate is only 5% for heaters with wicks in the high position. The data indicate that the fuel consumption rate, and hence the heat release rate, is directly proportional to wick position in the multi-stage heater. Reason for the greater deviation in the medium and low settings will be discussed subsequently. As the wick height is reduced, less fuel is delivered for evaporation and combustion, thus reducing the heat release rate. The range of adjustment in heating rate is seen from the data to be approximately 20 percent, which is lower than the manufacturer's specification of 30%. The average heat release rate (15,600 kJ/hr) for this multi-stage heater is 16% lower than the manufacturer's claim of 18,500 kJ/hr. The radiant heater (rated at 10,100 kJ/hr) and the convective heater (rated at 13,800 kJ/hr) are found to be similarly low (11% and 16% respectively) at their maximum wick settings.

Emissions in the heater exhaust were also examined at different positions in the manifold to test for uniformity of mixing. Measurements of combustion product gases at different radial and axial positions were found to be most uniform with the multi-stage heater and less for the convective design. The radiant heater was least uniform because it is designed to radiate heat outward, rather than allowing it to rise uniformly upward by convection.

When the multi-stage heater was relatively new, a set of experiments was performed to ascertain the effect of different wick heights on combustion. Experiments performed using the multi-stage heater yielded heat release rates closer to manufacturer's specifications. The variation in wick height between

the low and high positions produced differences in heat release rates of 30% in accord with the manufacturer's specification. When experiments of this type were repeated several months later, using the same but aged wick, it was not possible to reproduce the earlier results. Wick aging effects the burning rate and emission concentrations. Exhaust measurements for the multi-stage heater operating with a newer wick are summarized in Table IV, and those for the same heater with an aged wick are given in Table V. Carbon monoxide was measured with the NDIR analyzer for the experiments with the aged wick. Samples for all the exhaust measurements were extracted from the topmost port of the exhaust manifold, with the probe positioned along the centerline.

In Table IV the agreement between the measurements in the high wick position indicate that the experiments are very reproducible. The fuel consumption, CO_2 concentration, and NO concentration increase with wick height. The air dilution in the manifold expressed in terms of equivalence ratio decreases with increasing wick height since the combustion products are a larger part of the bulk flow.

For the first set of multi-stage exhaust measurements, a clear proportionality was indicated between wick height and fuel consumption, temperature, air-fuel equivalence ratio, CO_2, and NO. Table IV presents the data summarizing product compositions in the manifold when the wick was "young". Wick position alters the combustion zone appearance. There is an obvious lowering of the top of the flame zone from the third stage, down into the top of the second stage as the wick height is decreased. Aside from the dilution effects, the consistency of the composition data indicates that there is no change in combustion stoichiometry, within experimental error.

Fuel consumption and flame appearance are also influenced by the amount of fuel in the tank. Most experiments were performed when the fuel tank was neither filled to capacity nor nearly empty. One experiment designated by a

superscript "a" in Table V was performed with the tank completely full and the wick in the high position, and fuel consumption was greatest under these conditions. Another experiment designated by superscript "b" was performed under conditions where the tank was nearly empty and the wick was in the medium position, and fuel consumption is lowered by these conditions. In general the newer the wick, the greater the fuel consumption for a given wick setting. Filling the tank to capacity increases fuel consumption.

Table VI summarizes data for CO, NO and NO_2, taken for the multi-stage heater. The data are given in descending order of fuel consumption, and include data for aged wicks, different wick heights, and different amounts of fuel in the tank. Emission rates (microgram per kilojoule) are calculated from the measured fuel consumption rate, compositions of the dilute product stream, and the measured manifold temperature and pressure. Entries for emissions are shown both uncorrected and corrected for the ambient concentrations present in the laboratory during each experiment. The uncorrected CO data indicate an increase in the CO concentration with decreasing fuel consumption. When the data are corrected for ambient concentrations, CO concentrations, determined when heater fuel consumption was in excess of 12,500 kJ/hr, appear to be unaffected by fuel consumption rate; however the CO emissions are still highest for the lowest value of the fuel consumption rate. The NO concentration varies directly with fuel consumption rate. This is illustrated in Figure 5 where NO emissions expressed in terms of micrograms/kilojoule fuel are plotted against fuel consumption. A straight line is drawn through the data for clarity and to indicate the approximate linear relationship. The dependence of NO on fuel consumption is nearly first order behavior. The measured NO_2 concentrations show a curious lack of systematic behavior. Total NO_x does not vary significantly with total fuel consumption. Some preliminary data from the

multi-stage heater indicate that SO_2 at low ppm concentrations is found in the heater exhaust. Calculated values for SO_2 in the multi-stage heater, based upon the sulfur concentration in the fuel, are 3 ppm. Our measurements will be refined and comparison with calculated values will be made.

Tables VII and VIII contain a summary of the combustion characteristics of all three heaters. The amount of air dilution in the exhaust stack, as indicated by the values of equivalence ratio, is inversely related to the fuel consumption rate. The amount of CO_2 emitted to the exhaust per kilojoule heat output is listed for the heaters, and is based upon measured CO_2 concentrations, O_2 concentrations, N_2 concentrations, flow rates, and fuel consumption rates. If one assumes complete combustion and the stoichiometry given in Eq. 1, the CO_2 emissions rate can be calculated to be equal to 73,000 micrograms CO_2 per kilojoule fuel consumed. The experimentally determined values for CO_2 for the multi-stage heater agree with the calculated values to within 5%, and the experimentally determined CO_2 values for the convective heater agree with the calculated value to within 7%. Agreement is less satisfactory for the radiant heater, and we attribute this to greater uncertainties in the measured exhaust flow rates.

Table VIII summarizes the measurements of concentrations of the noxious pollutants: CO, NO and NO_2. All measurements are normalized to fuel consumption. The measured CO concentrations were largest for the radiant heater, and smallest for the multi-stage heater. The multi-stage heater is designed with a third stage which allows products of incomplete combustion time for further oxidation. In this stage there are elevated temperatures and sufficient residence time to assure the nearly complete burnout of CO to CO_2. Measured NO concentrations are greatest for the convective heater and least for the radiant heater; measured NO_2 concentrations for each of three heaters are similar. Total NO_x follows the same order with respect to heater type as

observed for NO. Since the fuel analysis indicated no measureable fuel nitrogen content, one must assume that the NO is formed from the thermal Zeldovich mechanism, and that the flame temperature must be the important variable which determines the extent of NO production. Since the air entrainment and hence dilution factors at various stages of the combustion process are different for the three heaters, and since combustion occurs throughout the heater, variations in flame temperatures must also occur. Additionally, radiant heat loss during the initial stages of combustion in the multistage and radiant heaters, could serve to reduce peak temperatures in the burnout region downstream. It is important to question whether or not NO_2 is actually present or is an artifact of sampling. It has been pointed out (Cernansky, 1977) that sampling from relatively cool post flame regions where radical concentrations are not significant, should result in no sample modification due to radical reactions within the sampling system. A possible explanation for the existence of NO_2 in the exhaust manifold is that it is formed near the combustion zone upstream from the exhaust, from turbulent mixing of cold dilution air with the combustion products. The mixing process involves the entrainment of cold air which quenches radicals, and allows the NO_2 to form from radical reactions with NO. The formation of NO_2 from NO under combustion conditions has been verified experimentally by Cernansky and Sawyer (Cernansky, 1975). In addition, the results of chamber studies of kerosene heaters indicate reasonably large concentrations of NO_2.

We have converted our detected emission rates to steady state concentrations in a chamber of fixed ventilation rate using a technique given by Traynor et al. (Traynor, 1982). It has been assumed that all comparisons are made for a constant value of the heat output rate (kJ/hr), and our measurements and those of others have been scaled accordingly. The following expression was

used to determine the equivalent steady state concentrations:

$$(X_i)_{ss} = \frac{1}{\rho_i} \frac{Q}{\dot{V}} E_i \tag{2}$$

where E_i = emission rate of species i (μg_i/kJ)

Q = common energy release rate (kJ/hr)

$\dot{V}$ = volumetric air flow rate (m^3_{air}/hr)

ρ_i = density of i at S.T.P. ($\mu g_i/m^3_i$)

X_i = column fraction of i (m^3_i/m^3_{air})

values chosen for Q = 8080 kJ/hr and $\dot{V}$ = 13.5 m^3/hr

The steady state concentrations are then compared with the results of environmental chamber studies (Leaderer, 1982; Traynor, 1983) and one laboratory study (Yamanaka, 1979). Our own results and those of others are summmarized in Table IX. The general results observed by other investigators concur with our own findings. The radiant heater emits greater concentrations of CO than the other types of heater. The reported CO concentrations range from 30 to 70 ppm. Although each of these heaters has a different heat release rate, the indicated steady state values, are normalized to a heater of 8080 kJ/hr heat output. It is also likely that the heaters of a given type are fabricated by different manufacturers and differ in design subtleties. The NO steady state concentrations are greatest for the convective heater, and least for the radiant heater. The radiant heater loses significant heat by radiation to the room, and as a result, the temperature in regions where NO formation occurs is less, and yields a corresponding reduction in NO formation. There is some disagreement among investigators regarding NO_2 concentrations emitted from

the convective heater; however, trends in total NO_x concentrations are in agreement for radiant and convective heaters.

Although there are no standards for indoor air, the CO concentrations emitted by the radiant heater do exceed standards for outdoor ambient air. All heaters exceed the California short-term (1 hr.) standard for NO_2 (Traynor, 1983). Without sufficient ventilation, carbon dioxide concentrations are of concern in all combustion appliances.

IV. SUMMARY AND CONCLUSIONS

The combustion characteristics of radiant, convective, and multi-stage kerosene heaters have been determined and compared. Two types of experiments were conducted. In the first of these, compostion and temperature were measured as a function of axial position in the heater to determine the progress of combustion. In the second type, composition, fuel consumption rate, temperature, pressure, and exhaust stream mass flow rate were measured in an exhaust manifold to ascertain the effect of heater type and heater operating conditions on exhaust gas composition. Fuel consumption was sensitive to wick height, wick age, and volume of fuel in the tank. Heater design strongly influenced emission concentrations. The multi-stage heater had the smallest concentration of CO and intermediate concentrations of NO_x. The radiant heater had the largest concentrations of CO and smallest NO_x concentrations. The convective heater had the greatest NO_x concentrations. Results were compared with chamber and other laboratory studies, and agreement among the various studies was found to be quite satisfactory.

ACKNOWLEDGEMENTS

This research was supported by the Assistant Secretary of Conservation and Renewable Energy, Office of Energy Systems Research, Energy Conservation and Utilization Technology Division of the U.S. Department of Energy, under Contract No. DE-AC03-76SF00098.

References

Cernansky N.P., Sawyer R.F. (1975) NO and NO_2 formation in a turbulent hydrocarbon/air diffusion flame, Fifteenth Symposium (International) on Combustion, The Combustion Institute, Pittsburgh, pp. 1039-1050.

Cernansky N.P., Sampling and measuring for NO and NO_2 in combustion systems, Experimental Diagnostics in Gas Phase Combustion Systems, Progress in Astronautics and Aeronautics, **53**, ed. B.T. Zinn, New York, pp. 83-102.

Clarkson S.G., Tom B.L., Babcock A.J., Mehkeri K.A. (1984) Results of testing unvented kerosene heaters in a house: gas emissions, surface temperatures and fuel consumption rates. Paper number 84-32.4 presented at the 77th annual meeting of the Air Pollution Control Association in San Francisco, CA, 24-29 June.

Kweller E.R. and Cuthrell G. (1980) Ventilated room combustion test results for three portable kerosene heaters, Consumer Product Safety Commision Report, National Bureau of Standards, Washington D.C.

Leaderer B.P. (1982) Air pollutant emissions from kerosene space heaters, Science, 218, 1113-1115.

Leaderer B.P., Stolwijk J.A.J., Zagraniski R.T., Qing-Shan M. (1984) A field study of indoor air contaminant levels associated with unvented combustion sources, Paper number 84-33.3 presented at the 77th annual meeting of the Air Pollution Control Association in San Francisco, CA, 24-29 June.

Lucas D., Morrow M.D., Brown, N.J. (1984) Measurement of sulfur dioxide in the post-combustion environment, Paper number 141 presented at the Twentieth Symposium (International) on Combustion in Ann Arbor, MI, 12-17 August.

Traynor G.W., Anthon D.W., Hollowell C.D. (1982) Technique for determining pollutant emissions from a gas-fired range, Atmospheric Environment, **16**,

2979-2987.

Traynor G.W., Allen J.R., Apte M.G., Girman J.R., Hollowell C.D. (1983) Pollutant emissions from portable kerosene-fired space heaters, Environmental Science and Technology, 17, 369-371.

Yamanaka S., Hirose G. and Takada S. (1979) Nitrogen oxides emissions from domestic kerosene-fired and gas-fired appliances. Atmospheric Environment, 13, 407-412.

Yamanaka S. (1984) Decay rates of nitrogen oxides in a typical japanese living room. Environmental Science and Technology, 18, 566-570.

LIST OF TABLES

I. Axial profile of species composition within the multistage heater. Species probing locations are indicated in Figure 3. Equivalence ratio (ϕ) is estimated from measured O_2 and N_2, assuming complete combustion.

II. Axial symmetry of species measurements inside the third stage of the multistage heater. Composition measurements are reported for two elevations and three tangential positions.

III. Summary of fuel consumption rate measurements for the various experiments. Mean values and standard deviations are tabulated.

IV. Exhaust measurements as a function of wick height for the multistage heater with a young wick. Carbon monoxide in concentrations greater than ten ppm was not detected.

V. Exhaust measurements as a function of wick height for the multistage heater with an older wick. Species reported are the stable (non-noxious) products of combustion. Variations in measurements with extreme fuel tank levels are included.

VI. Exhaust measurements as a function of wick height for the multistage heater with an older wick. Noxious pollutant species are tabulated, with and without correction for ambient background levels of the species.

VII. Comparison of measured fuel consumption and carbon dioxide emission rates for three heaters. Carbon dioxide emission rate is determined from exhaust measurements of concentration and flow velocity.

VIII. Summary of exhaust measurements for three heaters. Exhaust composition measurements and calculated emission rates are reported.

IX. Comparison of steady state indoor pollutant levels. Steady state concentrations are derived from emission rates of the various heaters assumed to be operating at a given heat release rate, in a chamber of fixed size and ventilation rate.

TABLE I

Multi-Stage Heater Axial Profile

Position[a] (cm)	ϕ[b]	hydro-carbons (%)	CO_2 (%)	O_2 (%)	N_2 (%)	CO (%)	NO_x (ppm)	NO_2 (ppm)	NO (ppm)	Temp (K)
1		0.114	~ 5.19	~ 10.0	~ 65.1	~ 0.366	16.9	8.5	8.4	
2	2.64	0.0016	5.23	13.4	75.4	0.019	21.8	13.5	8.2	1080
3[c]	14.1	*N.D.*[d]	0.98	19.1	75.7	0.016	1.5	0.1	1.4	1210
4		0.0201	12.0	2.77	77.9	1.40	18.8	2.1	16.6	1330
5	2.20	N.D.	6.40	11.6	77.3	0.049				
6	1.99	N.D.	7.06	10.9	76.8	N.D.	11.9	1.6	10.2	
7	2.02	N.D.	7.04	11.2	77.9	N.D.	10.0	N.D.	10.2	
8	1.92	N.D.	7.18	10.4	75.6	N.D.	12.6	2.0	10.5	
9	1.84	N.D.	7.56	9.94	76.0	N.D.				950

(a) See Figure 3

(b) $(\text{Air/Fuel})/(\text{Air/Fuel})_{\text{Stoichiometric}}$, estimated from measured O_2 and N_2 and assuming complete combustion

(c) Outside of flame contour, in flow of dilution air

(d) Non-Detectable

TABLE II

Symmetry of Product Composition Inside Third Stage

Position	ϕ	CO_2 (%)	O_2 (%)	N_2 (%)
Near third stage top	1.84	7.56	9.94	76.0
Rotated 90°	1.75	8.05	9.81	77.2
Above third stage flame	2.02	7.04	11.16	77.9
Rotated 90°	1.85	7.53	10.03	76.6
Rotated 180°	1.79	7.85	9.76	76.7

TABLE III

Summary of Fuel Consumption Rates

Heater and Wick Position	Number of Data	Fuel Consumption Rate (g/hr)	Heat Release[a] Rate (kJ/hr)	Manufacturer's Rating (kJ/hr)
Radiant - high	3	191 ± 6	8,250 ± 260	10,100
Convective - high	3	258 ± 13	11,100 ± 560	13,800
Multi-stage - high	15	360 ± 14	15,600 ± 600	18,500
- medium	4	320 ± 26	13,800 ± 1120	
- low	5	299 ± 27	12,900 ± 1170	

(a) Kerosene heat content = 43.2 kJ/g; 1.000 kJ/hr = 0.948 BTU/hr

TABLE IV

Multi-Stage Heater Exhaust Measurements

Wick Height	Fuel Consumption (g/hr)	CO_2 (%)	O_2 (%)	N_2 (%)	ϕ	Exhaust Temperature (K)	NO (ppm)	NO_2 (ppm)
high	356	1.65	18.4	76.8	8.4	490	2.4	*N.D.*[a]
high	348	1.67	18.5	77.5	8.4	490	2.4	N.D.
middle	303	1.56	18.8	78.0	9.1	470	1.9	0.1
low	271	1.44	18.7	77.0	9.7	450	1.5	0.2

(a) Non-Detectable

TABLE V

Multi-Stage Heater Exhaust Measurements

Wick Height	Fuel Consumption (g/hr)	CO_2 (%)	O_2 (%)	N_2 (%)	ϕ	Exhaust Temperature (K)
high[a]	370	1.39	19.9	77.8	10.3	460
high	342	1.41	19.3	78.0	10.1	470
high	338	1.40	19.1	78.3	10.2	450
low	323	1.28	20.0	78.2	11.2	440
low	316	1.46	19.2	80.1	10.0	440
med[b]	294	1.36	19.2	78.2	10.4	450
low	269	1.14	19.6	78.4	12.5	450

(a) Fuel tank completely full at beginning of experiment

(b) Very low fuel level and low flame at end of experiment

TABLE VI

Multi-Stage Heater Exhaust Measurements

Wick Height	Fuel Consumption (kJ/hr)	CO μg/kJ (ppm) (a)	CO μg/kJ (ppm) (b)	NO μg/kJ (ppm) (a)	NO μg/kJ (ppm) (b)	NO_2 μg/kJ (ppm) (a)	NO_2 μg/kJ (ppm) (b)
high[c]	16,000	2.4 (0.7)	1.7 (0.5)	7.5 (2.1)	7.2 (2.0)	4.3 (0.8)	2.3 (0.4)
high	14,800	4.6 (1.4)	1.0 (0.3)	6.0 (1.7)	5.6 (1.6)	m.e.[e]	m.e.
high	14,600			5.7 (1.6)	5.2 (1.5)	5.6 (1.0)	2.5 (0.5)
low	13,900	4.0 (1.1)	2.2 (0.6)	6.1 (1.6)	5.7 (1.5)	4.3 (0.7)	2.2 (0.4)
low	13,700	3.8 (1.2)	2.2 (0.7)	5.9 (1.7)	5.5 (1.6)	4.2 (0.8)	2.9 (0.6)
med[d]	12,700	7.9 (2.3)	2.7 (0.8)	4.9 (1.3)	4.4 (1.2)	4.4 (0.8)	2.2 (0.4)
low	11,600	18 (4.4)	7.4 (1.8)	4.7 (1.1)	4.0 (0.9)	7.7 (1.1)	3.2 (0.5)

(a) As measured in exhaust, per fuel consumed

(b) Corrected for ambient concentrations, per fuel consumed

(c) Fuel tank completely full at beginning of experiment

(d) Very low fuel level and low flame at end of experiment

(e) Measurement error

TABLE VII

Comparison of Heaters

Heater[a]	Fuel Consumption (kJ/hr)	ϕ[b]	CO_2 (μg/kJ)	CO_2 (%)	Temperature[b] (K)
Radiant	8,040	12.8	85,000	(1.11)	390
	8,160	13.8	81,000	(1.05)	400
Convective	11,300	10.5	78,000	(1.37)	440
	11,600	11.1	76,000	(1.29)	430
Multi-stage	14,800	10.1	72,000	(1.41)	470
	14,600	10.2	75,000	(1.40)	450
	16,000	10.3	77,000	(1.39)	460

(a) All measurements performed with wick in high position

(b) $(\text{Air/Fuel})/(\text{Air/Fuel})_{\text{stoichiometric}}$, estimated from measured O_2 and N_2 and assuming complete combustion

(c) Measured in exhaust. CO_2 emission rate (μg/kJ) determined from exit velocity

TABLE VIII

Comparison of Heaters

Heater[a]	Fuel Consumption (kJ/hr)	Emissions[b] CO (μg/kJ)	CO (ppm)	NO (μg/kJ)	NO (ppm)	NO_2 (μg/kJ)	NO_2 (ppm)
Radiant	8,160	130	(29.3)	1.7	(0.4)	5.6	(0.8)
Convective	11,600	8.0	(2.2)	16.3	(4.2)	5.6	(0.9)
Multi-stage	14,800	4.6	(1.4)	6.0	(1.7)	m.e.[c]	m.e.
	14,600			5.7	(1.6)	5.6	(1.0)
	16,000	2.4	(0.7)	7.5	(2.1)	4.3	(0.8)

(a) All measurements performed with wick in high position

(b) Measured in exhaust. Emission rate (μg/kJ) calculated from determined from Fuel consumption rate

(c) Measurement error

TABLE IX

Steady State Indoor Pollutant Levels

Study	Heater	Heat Release Rate (kJ/hr)	CO (ppm)	NO (ppm)	NO_2 (ppm)	NO_x (ppm)
A[a] (Lionel)	Multi-stage	15,100	1.8	3.1	1.8	4.9
	Convective	11,600	4.2	8.0	1.8	9.8
	Radiant	8,160	68.3	0.8	1.8	2.6
B (Leaderer, 1982)	Convective	5,870	11.7	5.7	4.6	10.3
	Radiant	6,760	30.6	<0.1	1.6	1.6
C (Traynor, 1983)	Convective	7,850	4.8	12.2	4.1	16.3
	Radiant	8,250	37.6	0.6	1.3	1.9
D (Yamanaka, 1979)	Convective	8,070				21.6
	Radiant	9,430				2.9
Health Standards			35[b]		0.25[c]	

(a) Data calculated from heater exhaust measurements

(b) E.P.A. ambient air quality standard for CO (1 hr. average not to be exceeded more than once a year)

(c) California short-term (1 hr.) standard for NO_2

LIST OF FIGURES

Figure 1. Schematic diagram of experimental apparatus: C.L.A. chemiluminescence analyzer; G.C. gas chromatograph; N.D.I.R. non-dispersive infra-red analyzer.

Figure 2. Schematic diagram indicating an exploded view of the combustion chamber of the multi-stage heater.

Figure 3. Schematic diagram showing the axial probing positions in a cross-section of the multi-stage heater. The flaming combustion zone is indicated by wavy lines which pass through position 4.

Figure 4. Temperatures in (^{o}C) as a function of distance from the centerline (cm) of the exhaust stack, measured with a 0.10 cm diameter inconel sheathed chromel-alumel thermocouple. Symbols represent insertion through the top left port (O) or top right port (△); maximum typical uncertainty is 20°.

Figure 5. Nitric Oxide concentrations in (g/kJ) as a function of fuel consumption in (kJ/hr). The probe is located at the centerline of the exhaust manifold. Symbols represent the multi-stage heater (O), the radiant heater (△), and the convective heater (□).

Figure 1

EXPERIMENTAL APPARATUS

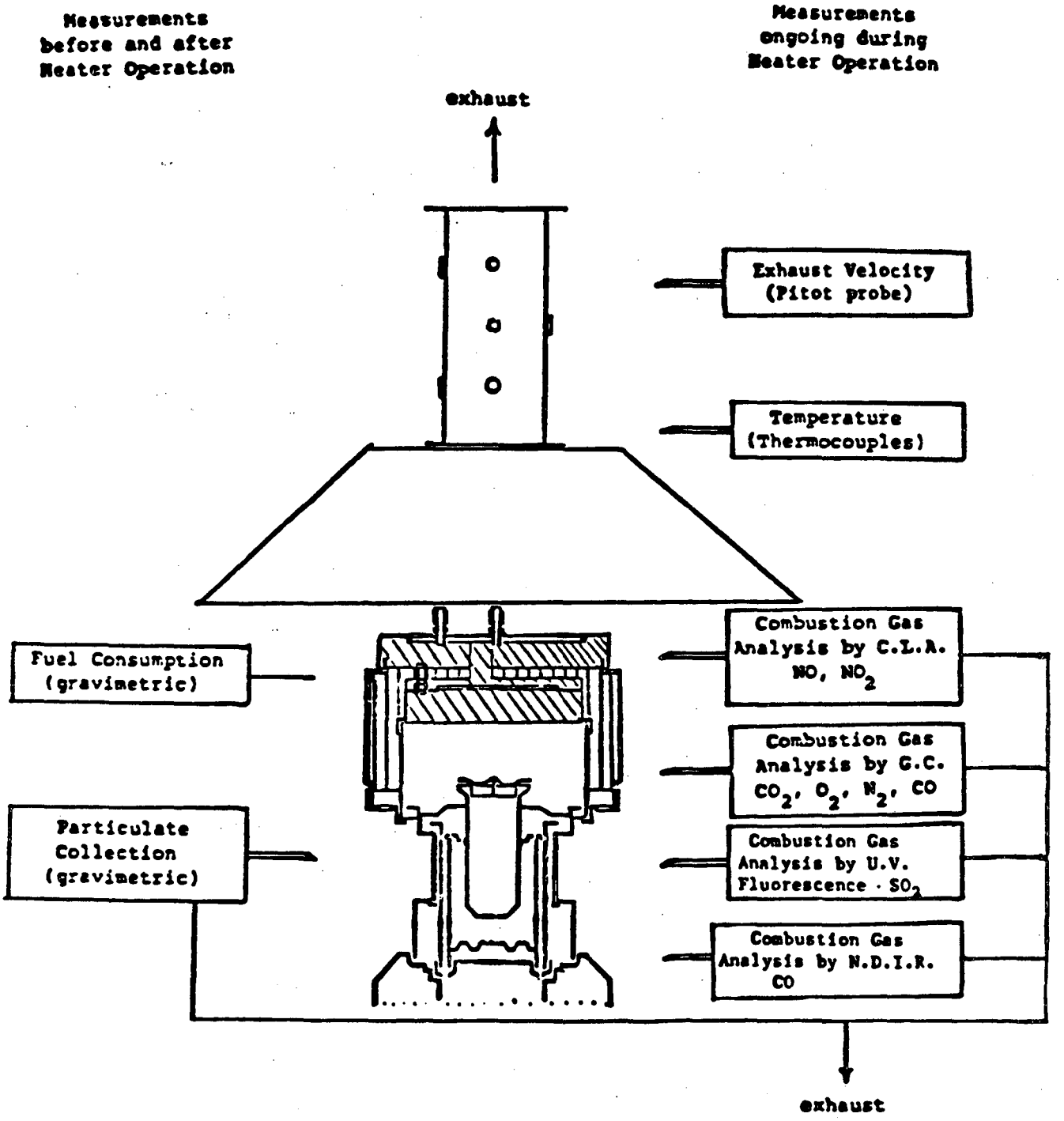

Figure 2

COMBUSTION CHAMBER

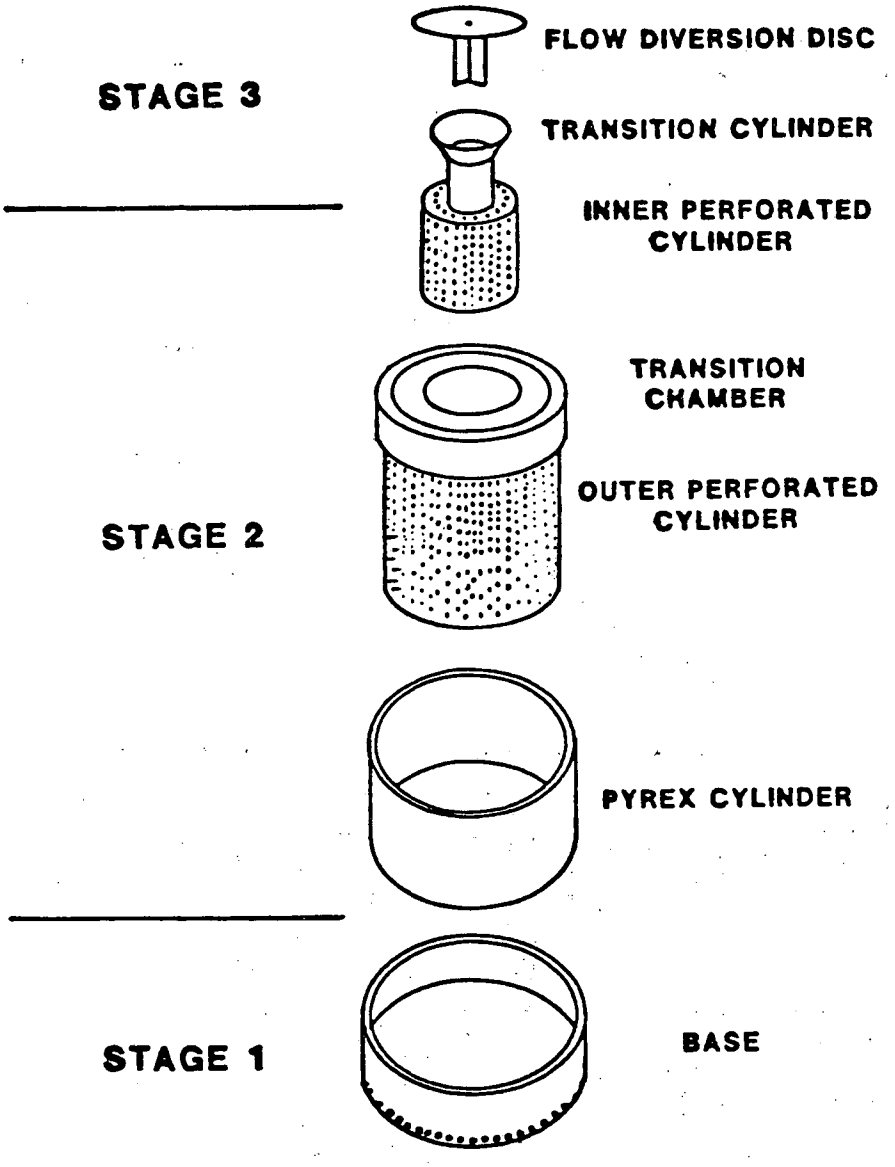

Figure 3

AXIAL PROBING POSITIONS IN THE MULTI-STAGE HEATER

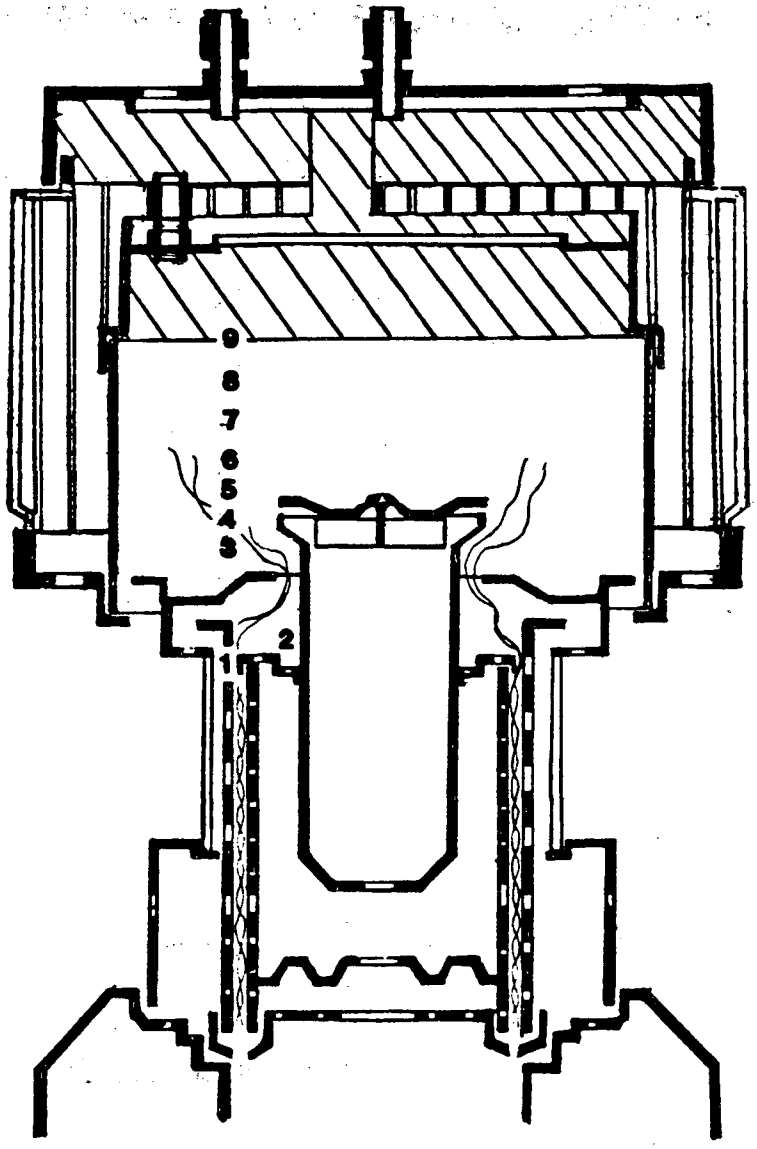

Figure 4

TEMPERATURE PROFILE IN EXHAUST STACK

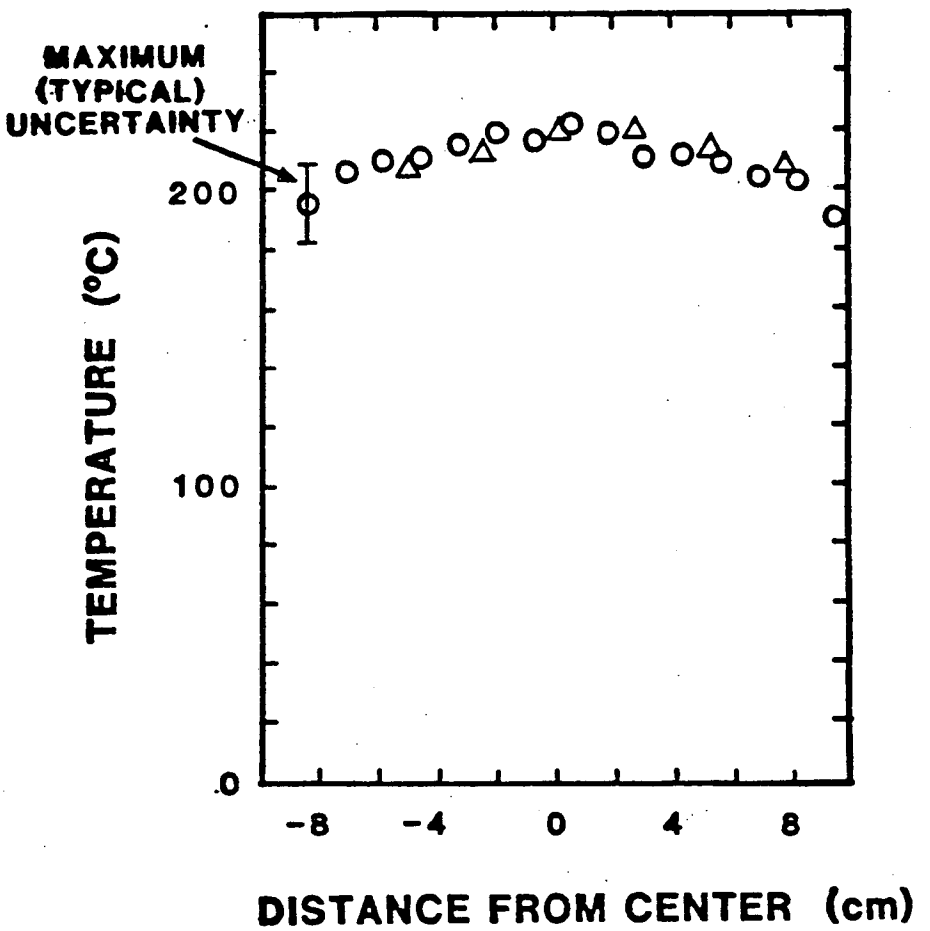

Figure 5

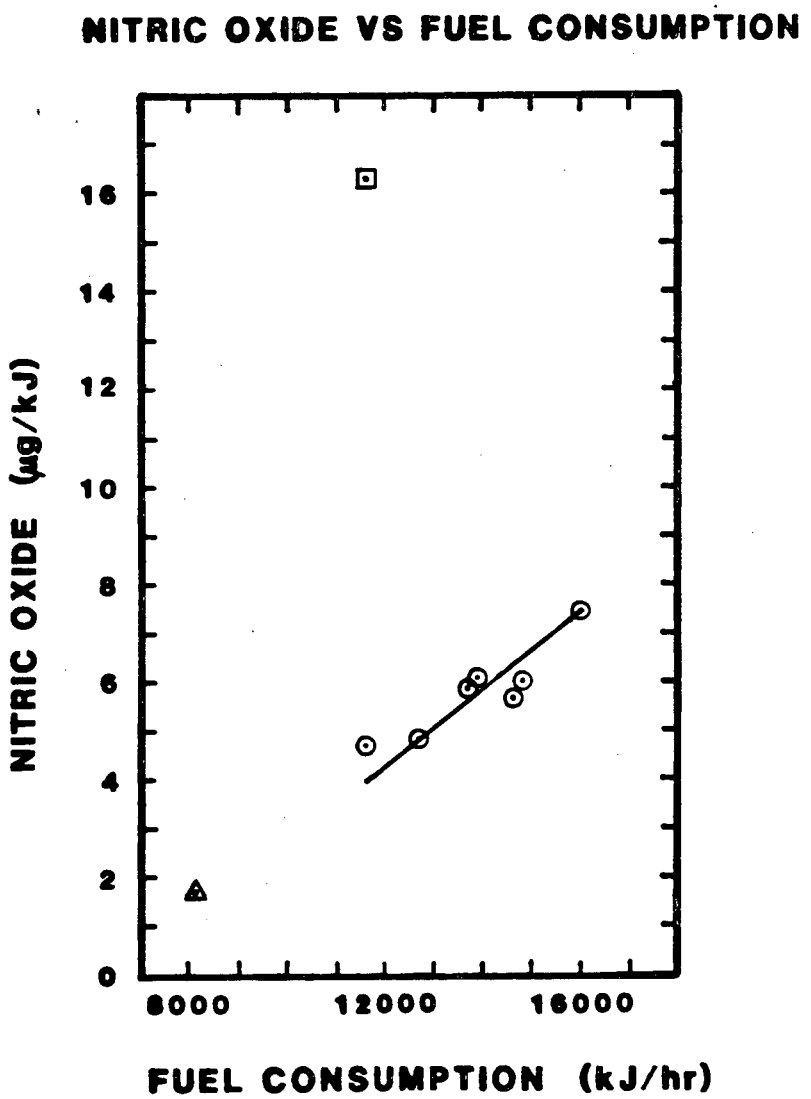
NITRIC OXIDE VS FUEL CONSUMPTION
NITRIC OXIDE (µg/kJ)
0
2
4
6
8
10
12
14
16
8000
12000
16000
FUEL CONSUMPTION (kJ/hr)

This report was done with support from the Department of Energy. Any conclusions or opinions expressed in this report represent solely those of the author(s) and not necessarily those of The Regents of the University of California, the Lawrence Berkeley Laboratory or the Department of Energy.

Reference to a company or product name does not imply approval or recommendation of the product by the University of California or the U.S. Department of Energy to the exclusion of others that may be suitable.

TECHNICAL INFORMATION DEPARTMENT
LAWRENCE BERKELEY LABORATORY
UNIVERSITY OF CALIFORNIA
BERKELEY, CALIFORNIA 94720